

SAM-DA: UAV Tracks Anything at Night with SAM-Powered Domain Adaptation

Liangliang Yao[†], Haobo Zuo[†], Guangze Zheng[†], Changhong Fu^{*}, Jia Pan

Abstract—Domain adaptation (DA) has demonstrated significant promise for real-time nighttime unmanned aerial vehicle (UAV) tracking. However, the state-of-the-art (SOTA) DA still lacks the potential object with accurate pixel-level location and boundary to generate the high-quality target domain training sample. This key issue constrains the transfer learning of the real-time daytime SOTA trackers for challenging nighttime UAV tracking. Recently, the notable Segment Anything Model (SAM) has achieved remarkable zero-shot generalization ability to discover abundant potential objects due to its huge data-driven training approach. To solve the aforementioned issue, this work proposes a novel SAM-powered DA framework for real-time nighttime UAV tracking, *i.e.*, SAM-DA. Specifically, an innovative SAM-powered target domain training sample swelling is designed to determine enormous high-quality target domain training samples from every single raw nighttime image. This novel one-to-many method significantly expands the high-quality target domain training sample for DA. Comprehensive experiments on extensive nighttime UAV videos prove the robustness and domain adaptability of SAM-DA for nighttime UAV tracking. Especially, compared to the SOTA DA, SAM-DA can achieve better performance with fewer raw nighttime images, *i.e.*, the fewer-better training. This economized training approach facilitates the quick validation and deployment of algorithms for UAVs. The code is available at <https://github.com/vision4robotics/SAM-DA>.

Index Terms—Segment anything model (SAM), domain adaptation, nighttime UAV tracking, high-quality training sample swelling, one-to-many generation, fewer-better training.

1 INTRODUCTION

OBJECT tracking has been applied for wide unmanned aerial vehicle (UAV) applications, *e.g.*, geographical research [1], dynamic object investigation [2], search and rescue mission [3], and visual location [4]. Using abundant daytime superior-quality tracking datasets [5], [6], [7], [8], [9], state-of-the-art (SOTA) trackers [10], [11], [12], [13] have attained remarkable performance. Nevertheless, the performance of these SOTA trackers is unsatisfactory in darkness due to the limited illumination, low contrast, and much noise of nighttime images in comparison to daytime ones [14], [15]. The aforementioned distinctions bring the discrepancy in feature distribution between day and night images. A potential solution is capturing and annotating sufficient nighttime data for directly training effective nighttime trackers. However, it is expensive and time-consuming to label a large amount of high-quality tracking data under unfavorable lighting conditions.

Considering the labeling cost of the nighttime image and the domain gap of day-night, domain adaptation [16] is introduced to solve the problem of nighttime UAV tracking. This method aims to transfer SOTA trackers developed for daytime situations to nighttime UAV tracking. In the source domain, the training data has well-annotated bounding boxes with high expenses by hand, whereas, in the target domain, the training samples are obtained by the automatic method [17] instead of manual annotation. However, the

insufficient quality of target domain training samples limits the improvement of domain adaptation. The generation approach of training samples has difficulty extracting the potential object with precise pixel-level location and boundary from challenging nighttime images of UAV perspectives [18]. Furthermore, this method solely concentrates on one target domain training sample within a single nighttime image, disregarding abundant other valuable potential objects, *i.e.*, one-to-one generation. *Therefore, how to generate enormous and high-quality target domain training samples from every single raw nighttime image for robust day-night domain adaptation is an urgent problem.*

Recently, the Segment Anything Model (SAM) [19] has demonstrated an impressive zero-shot generalization capacity, allowing it to uncover numerous potential objects. This achievement can be attributed to its huge data-driven training approach with over one billion masks. Such kind of generalization ability enables SAM to be directly applied for various vision-based tasks without task-oriented training, including camouflaged object detection [20], image inpainting [21], medical image segmentation [22], *etc.* Moreover, with the enormous parameters, the image encoder of SAM is capable of extracting the robust image features in various environments. Despite the above advantages, SAM is hard to be directly applied for nighttime UAV tracking due to the limited load source and computation power of the UAV. *Thereby, how to effectively utilize the considerable zero-shot generalization ability of SAM for real-time nighttime UAV tracking is worth being explored carefully.*

This work introduces the superb SAM into the training phase of tracking-oriented day-night domain adaptation for the first time, proposing a novel SAM-powered domain adaptation framework, *i.e.*, SAM-DA. Specifically,

- [†] Equal contribution. ^{*} Corresponding author.
- Liangliang Yao, Haobo Zuo, and Changhong Fu are with the School of Mechanical Engineering, Tongji University, Shanghai 201804, China E-mail: changhongfu@tongji.edu.cn
- Guangze Zheng and Jia Pan are with the Department of Computer Science, University of Hong Kong, Hong Kong 999077, China.

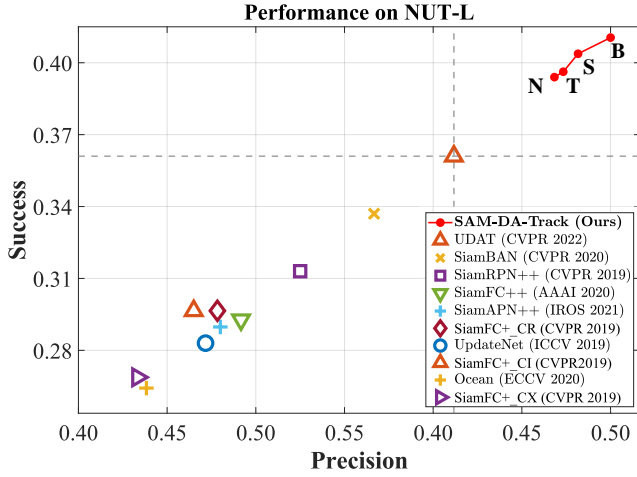


Fig. 1: Overall performance of SAM-DA-Track and state-of-the-art (SOTA) trackers on the proposed NUT-L. SAM-DA-Track represents the version of the base tracker (dubbed as SiamBAN [23]), adopting SAM-DA for adaptation training. N, T, S, B represent that the target domain training images of SAM-DA-Track are about 10.0%, 33.2%, 50.1%, and all of the entire NAT2021-*train* [16], respectively. With SAM, the proposed fewer-better training contributes to the superior performance of SAM-DA with only 10% of training images (denoted as N) of baseline (denoted as UDAT [16]).

the inventive SAM-powered target domain training sample swelling is presented to determine enormous high-quality target domain training samples from every single challenging nighttime image, dubbed the one-to-many generation. Thereby, the dependence on the number of raw images required for adaptation training can be reduced to enhance generalization and prevent overfitting. With the improvement and increase of target domain training samples, the adaptation effect of SOTA trackers for nighttime UAV tracking can be further boosted. Figure 1 shows the tracking performance comparison of SAM-DA-Track and other SOTA tracking methods on a comprehensive long-term nighttime UAV tracking benchmark, *i.e.*, NUT-L, which is a combination of long-term sequences from NAT2021-*test* [16] and UAVDark135 [24]. SAM-DA-Track symbolizes the version of the base tracker, *i.e.*, SiamBAN [23], using SAM-DA for adaptation training. N, T, S, B represent that the target domain training images of SAM-DA-Track are about 10.0%, 33.2%, 50.1%, and all of the entire NAT2021-*train*, respectively. The baseline is UDAT [16]. Compared to this method, SAM-DA-Track adopting the training framework SAM-DA can achieve superior tracking performance with less raw nighttime images, *i.e.*, the few-better training. The main contributions of this work are as follows:

- A novel SAM-powered domain adaptation framework, namely SAM-DA, is proposed for real-time nighttime UAV tracking. According to our knowledge, SAM-DA is the first work to combine SAM with domain adaptation for UAV tracking at night.
- An innovative SAM-powered target domain training sample swelling is designed to determine enormous high-quality target domain training samples from every single raw nighttime image.

- Comprehensive experiments on extensive nighttime videos verify the effectiveness and domain adaptability of SAM-DA for nighttime UAV tracking. Especially, SAM-DA realizes better performance with fewer raw images compared to the SOTA method. The above training approach promotes the quick validation and deployment of algorithms for UAVs.

2 RELATED WORK

2.1 Nighttime UAV tracking

Recently, nighttime UAV tracking has been utilized in a variety of practical applications, attracting widespread interest [25]. Initially, the tracking-oriented low-light enhancers [14], [15], [26] are designed to improve the nighttime tracking performance of the cutting-edge Siamese trackers [27], [28], [29], [30], [31]. Specifically, J. Ye *et al.* [14] develop an enhancer to iteratively mitigates the effects of inadequate illumination and noise. Afterwards, they present a spatial-channel Transformer-based low-light enhancer to achieve robust nighttime UAV tracking [15]. Besides, High-lightNet [26] is designed to illuminate potential objects for human operators and UAV trackers, improving the human-machine interaction. Nevertheless, this kind of plug-and-play method has a restricted relationship with tracking tasks, and the way to directly insert tracking models is unable to minimize the image feature distribution gap. In addition, the model parameters of the low-light enhancers will seriously increase the burden of the limited UAV computation and resource.

2.2 Day-night domain adaptation

Day-night domain adaptation has been used for a wide range of visual tasks [32], [33] because it can decrease the domain gap and transfer information from the source domain (daytime) to the target domain (nighttime). X. Wu *et al.* [32] train a domain adaptation model for semantic segmentation at night using adversarial learning. Y. Sasagawa *et al.* [33] use domain adaptation to combine deep learning models from various disciplines in order to detect nighttime objects. Despite the rapid development in other vision tasks, day-night domain adaptation still lacks research for object tracking. Thereby, UDAT [16] introduces unsupervised domain adaptation into nighttime UAV tracking, thus increasing the tracking performance at night. However, the insufficient quality of target domain training samples constrains the advancement of the domain adaptation performance for nighttime UAV tracking. Due to the challenges of nighttime images from UAV perspectives, the existing generation approach [17] of training samples struggles to extract the potential object with exact pixel-level location and boundary. In addition, this kind of approach only considers one target domain training sample inside a single nighttime image, ignoring abundant additional worthwhile potential objects.

2.3 Segment anything model

SAM [19] has found extensive use in many kinds of computer vision tasks as a huge data-driven method. Trained with over a billion masks, the renowned SAM has extraordinary zero-shot generalization ability. The above capability

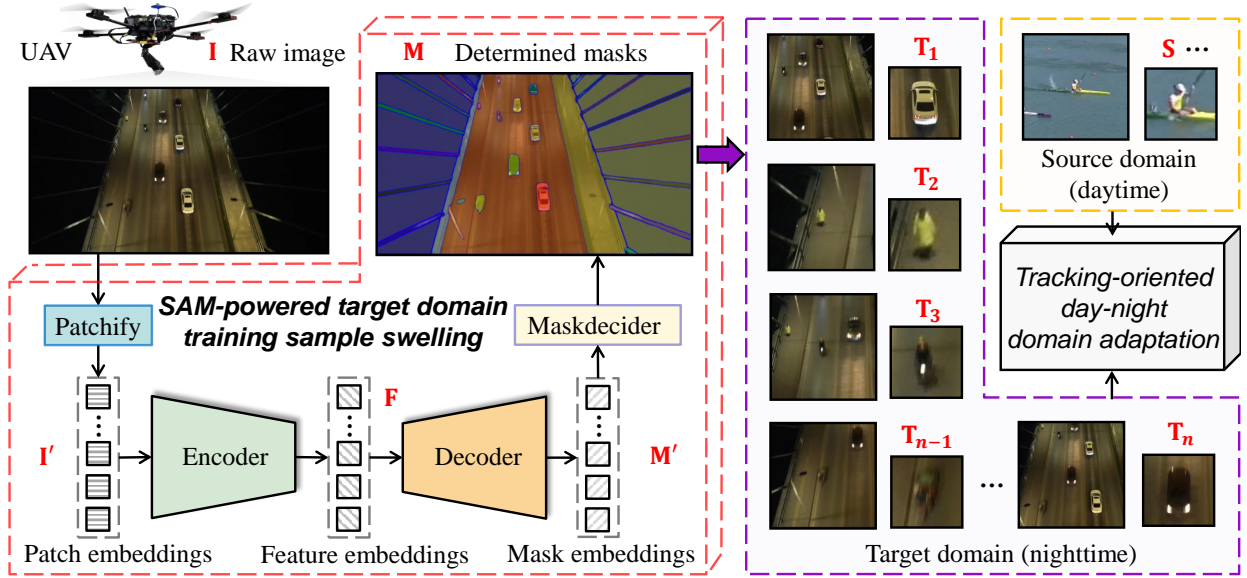


Fig. 2: Illustration of the proposed SAM-DA for nighttime UAV tracking. The original nighttime image is from NAT2021-train. The source domain training sample is from GOT-10k [6]. The SAM-powered target domain training sample swelling is employed to determine enormous high-quality target domain training samples from every single nighttime image. The purple arrow represents the crop operation to generate the swelled training samples. Note the source domain (daytime) training samples are manually collected with time-consuming and expensive annotation, while the target domain (nighttime) training samples is automatically generated with our time-saving and low-cost swelling.

allows SAM to be directly applied for different vision-based tasks. Specifically, L. Tang *et al.* [20] provide an initial assessment for the efficacy of SAM on the camouflaged object detection assignment. S. Roy *et al.* [22] seek to undertake an early assessment of the out-of-the-box zero-shot capabilities of SAM for medical image segmentation. Besides, T. Yu *et al.* [21] make the initial attempt at mask-free image inpainting and present a new paradigm of “clicking and filling” called Inpaint Anything, which is based on SAM. Despite its wide applications in other vision tasks, SAM has not been used for UAV tracking, especially in nighttime scenarios.

3 PROPOSED METHOD

SAM-DA is introduced in this section, as depicted in Fig. 2. Given a nighttime raw image, the SAM-powered target domain training sample swelling is employed to determine enormous potential objects and provide their accurate pixel-level locations and boundaries. Then, the number of training samples swells from one to many within every single nighttime image based on the location and boundary. During the training pipeline, both the manually annotated source domain (daytime) training sample and automatically generated target domain (nighttime) training sample are leveraged to drive the following tracking-oriented day-night domain adaptation. This data-driven framework introduces SAM into the training phase of domain adaptation, improving the performance of the tracker in the nighttime scene.

3.1 SAM-powered target domain training sample swelling

Effective day-night domain adaptation requires enormous high-quality target domain training samples. Different from the existing one-to-one approach [17], the proposed SAM-powered target domain training sample swelling utilizes the

powerful zero-shot generalization ability of SAM to swell the number of high-quality training samples. The detail is introduced as follows.

SAM-powered model. As shown in Fig. 2, the SAM-powered model is illustrated. Specifically, following the original SAM, a nighttime raw image $I \in \mathcal{R}^{H \times W \times 3}$ is first patchified to patch embedding I' . Subsequently, an encoder is utilized to extract feature embeddings denoted by F as follows:

$$\begin{aligned} I' &= \text{Patchify}(I) , \\ F &= \text{Encoder}(I') , \end{aligned} \quad (1)$$

where Patchify means that the image is projected linearly and added with position embeddings. Additionally, Encoder represents an MAE [34] pre-trained Vision Transformer (ViT) [35].

Afterward, a decoder predicts the mask embeddings M' . Then, a mask decoder generates the image with enormous determined masks M . The process is defined as:

$$\begin{aligned} M' &= \text{Decoder}(F) , \\ M &= \text{Maskdecoder}(M') , \end{aligned} \quad (2)$$

where Decoder is a modification of a Transformer decoder block [36] and Maskdecoder is a dynamic mask prediction head. These masks contain information about the potential object with accurate location and boundary. Hence, the boxes B_n around the masks are utilized to generate target domain training samples. n is the number of potential objects for a single nighttime image.

Remark 1: It is noted that the original SAM is difficult to be utilized straightforwardly for real-time nighttime UAV tracking due to the restricted load source and processing capabilities of the UAV. Therefore, this work adopts SAM to generate high-quality target domain training samples for day-night domain adaptation training.

Target domain training sample swelling. The target domain training sample swelling generates many high-quality training samples from one original nighttime image. Specifically, this work follows the data processing of COCO [7]. An image \mathbf{I} exhibits the dual functionality of serving as both a template frame and a search frame. As a template frame, the image is cropped into numerous target-centered image patches, denoted as template patches $[\mathbf{Z}_1, \mathbf{Z}_2, \dots, \mathbf{Z}_n]$, with the accurate locations and boundaries, which are subsequently resized to a fixed size (e.g., 127×127). Simultaneously, as a search frame, the image is cropped into an equal number of larger image patches, denoted as search patches $[\mathbf{X}_1, \mathbf{X}_2, \dots, \mathbf{X}_n]$, also based on the accurate locations and boundaries, and resized to another size (e.g., 255×255). Patches containing the same target are paired between the template patches and search regions patches, forming the target domain training samples \mathbf{T}_n . The whole target domain training sample swelling is defined as:

$$\begin{aligned} [\mathbf{Z}_1, \mathbf{Z}_2, \dots, \mathbf{Z}_n] &= \text{Crop}(\mathbf{I}; \mathbf{B}_i, s1) \quad , \\ [\mathbf{X}_1, \mathbf{X}_2, \dots, \mathbf{X}_n] &= \text{Crop}(\mathbf{I}; \mathbf{B}_i, s2) \quad , \\ \mathbf{T}_n &= \{ \{ \mathbf{Z}_1, \mathbf{X}_1 \}, \{ \mathbf{Z}_2, \mathbf{X}_2 \}, \dots, \{ \mathbf{Z}_n, \mathbf{X}_n \} \} \quad , \end{aligned} \quad (3)$$

where Crop is the crop operation to generate patches and \mathbf{B}_i is the box of the i -th potential object. Besides, $s1, s2$ represent template size and search size, respectively.

As shown in Fig. 3, the visualization represents the swelling method from one original nighttime image to many target domain training samples.

Remark 2: The one-to-many generation revolutionizes the existing target domain training sample acquisition approach in the day-night domain adaptation from both the aspects of quantity and quality.

3.2 Tracking-oriented day-night domain adaptation

With a substantial amount of high-quality target domain training samples, a tracking-oriented day-night domain adaption is utilized to enhance the trackers' nighttime performance by aligning the features from both domains. Following the baseline, the whole domain adaptation framework is divided into three parts: backbone, bridge layer, and discriminator.

Backbone. In a general Siamese network-based tracker, feature extraction involves two branches, the template branch and search branch. These branches utilize an identical backbone network \mathcal{F} to generate feature maps from the template patch \mathbf{Z} and search patch \mathbf{X} , namely $\mathcal{F}(\mathbf{Z})$ and $\mathcal{F}(\mathbf{X})$.

Bridging layer. In consideration of the strong modeling capability of the vision Transformer for long-range interdependencies, a bridging layer is designed as a Transformer structure to bridge the gap between the feature distributions [16]. Taking the search branch as an instance, positional encodings \mathbf{Pos} are added to the input feature $\mathcal{F}(\mathbf{X}) \in \mathcal{R}^{N \times H \times W}$. The subsequent operation is the multi-head self-attention (MSA), which can be expressed as:

$$\begin{aligned} \widehat{\mathcal{F}(\mathbf{X})}' &= \text{MSA}(\mathbf{Pos} + \mathcal{F}(\mathbf{X})) + \mathbf{Pos} + \mathcal{F}(\mathbf{X}) \quad , \\ \widehat{\mathcal{F}(\mathbf{X})} &= \text{LN}(\text{FFN}(\text{Mod}(\text{LN}(\widehat{\mathcal{F}(\mathbf{X})}')) + \widehat{\mathcal{F}(\mathbf{X})}') \quad , \end{aligned} \quad (4)$$

where $\widehat{\mathcal{F}(\mathbf{X})}'$ refers to an intermediate variable and LN represents layer normalization. Additionally, FFN denotes the fully connected feed-forward network. Mod is a modulation layer in [10] to fully explore internal spatial information.

Discriminator. A discriminator is employed to ascertain the origin of the modulated feature map, discerning whether they belong to the source domain or the target domain. The feature discriminator consists of a gradient reverse layer [37] and two Transformer layers. Given the modulated feature map $\widehat{\mathcal{F}(\mathbf{X})}$, the softmax function is performed and followed by a gradient reverse layer. Then the intermediate feature \mathbf{R} is passed through a convolution layer and concatenated with a classification token \mathbf{cls} as:

$$\begin{aligned} \mathbf{R} &= \text{GRL}(\text{Softmax}(\widehat{\mathcal{F}(\mathbf{X})})) \quad , \\ \mathbf{R}' &= \text{Concat}(\mathbf{cls}, \text{Conv}(\mathbf{R})) \quad , \end{aligned} \quad (5)$$

where GRL represents the gradient reverse layer and Concat denotes channel-wise concatenation.

Afterward, \mathbf{R}' is input to two Transformer layers. Finally, the classification token \mathbf{cls} is regarded as the final predicted result.

Tracker head. After the bridging layer, a cross-correlation operation is calculated on the modulated features $\widehat{\mathcal{F}(\mathbf{X})}$ and $\widehat{\mathcal{F}(\mathbf{Z})}$ to generate a similarity map. Finally, the tracker head performs the classification and regression process to predict the object position.

Remark 3: As shown in Fig. 4, visual comparison of confidence maps generated by the baseline, the SAM-DA-Track-N, the SAM-DA-Track-T, the SAM-DA-Track-S, and the SAM-DA-Track-B. With a substantial amount of high-quality target domain training samples, the tracking-oriented day-night domain adaptation greatly improve the performance of the tracker at night.

3.3 Loss functions

Following the baseline, the loss of the domain adaptation framework consists of tracking loss and domain adaptation loss.

Tracking loss. In the source domain, the tracking loss including classification and regression loss \mathcal{L}_{tr} between the manually-annotated ground truth and the predicted results are used.

Domain adaptation loss. In adversarial learning, the least-square loss function [38] is employed to train the generator \mathcal{G} , aiming at generating source domain-like features from target domain images to fool the discriminator \mathcal{D} while frozen. Here the feature extractor along with the bridging layer is regarded as the generator \mathcal{G} . Considering both the template and search features, the adversarial loss \mathcal{L}_{da} is described as follows:

$$\mathcal{L}_{\text{da}} = (\mathcal{D}(\widehat{\mathcal{F}(\mathbf{X}_t)}) - l_s)^2 + (\mathcal{D}(\widehat{\mathcal{F}(\mathbf{Z}_t)}) - l_s)^2 \quad , \quad (6)$$

where s and t refer to the source and the target domains, respectively. Besides, l_s represents the label for the source domain.

In summary, the total training loss for the domain adaptation framework is defined as:

$$\mathcal{L}_{\text{total}} = \mathcal{L}_{\text{tr}} + \lambda \mathcal{L}_{\text{da}} \quad , \quad (7)$$

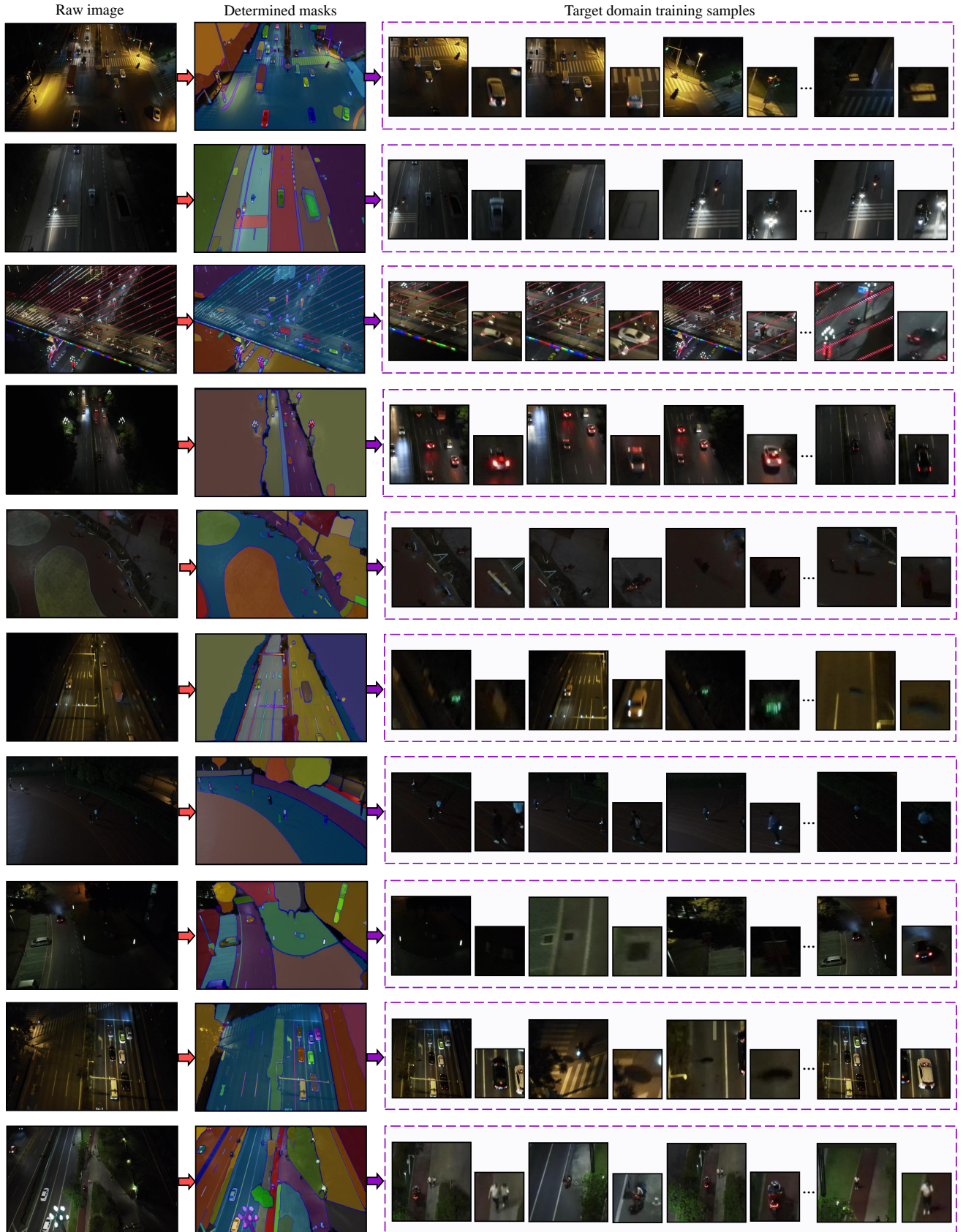


Fig. 3: Visualization of the target domain training samples processed by the SAM-powered target domain training sample swelling. The nighttime raw images are from NAT2021-*train*. With the novel one-to-many generation, many objects, such as buses, cars, riders, and signals are utilized to generate the training samples from a single image, enhancing the utilization efficiency of the raw nighttime data.



Fig. 4: Visual comparison of confidence maps generated by the baseline, the SAM-DA-Track-N, the SAM-DA-Track-T, the SAM-DA-Track-S, and the SAM-DA-Track-B. Target objects are marked by **red** boxes. The nighttime images are from the proposed NUT-L. The baseline demonstrates poor performance when tracking in long videos captured under low-light conditions. In contrast, the proposed SAM-DA-Track exhibits a substantial enhancement of the tracker’s capabilities owing to the utilization of abundant high-quality target domain training samples.

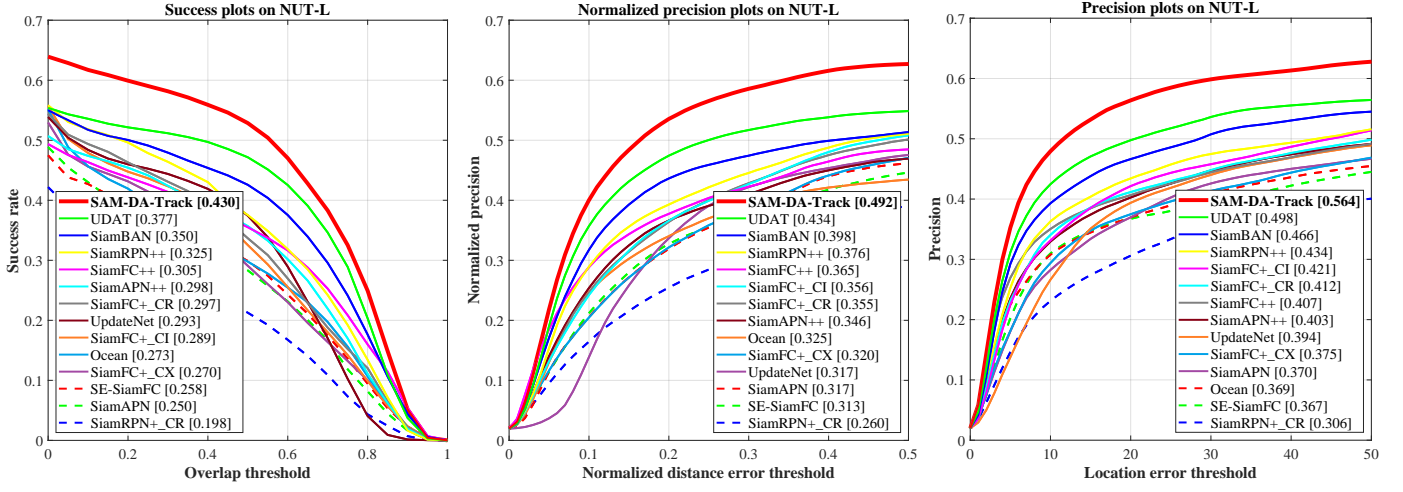


Fig. 5: Overall performance of SAM-DA-Track and SOTA trackers on NUT-L. SAM-DA-Track significantly surpasses the baseline and other SOTA methods.

where λ is a weight to balance the loss terms. λ is set as 0.01 in implementation.

During the training process, the tracking network and discriminator \mathcal{D} are optimized alternatively. The loss function of the discriminator \mathcal{D} is defined as:

$$L_{\mathcal{D}} = \sum_{d=s,t} (\mathcal{D}(\widehat{\mathcal{F}}(\mathbf{X}_d)) - l_d)^2 + (\mathcal{D}(\widehat{\mathcal{F}}(\mathbf{Z}_d)) - l_d)^2 \quad . \quad (8)$$

4 EXPERIMENTS

4.1 Implementation details

Data. SAM-powered target domain training sample swelling is mainly implemented on NAT2021-*train* to validate the influence of target domain training samples' quantity and quality on nighttime tracking performance. To validate the effectiveness of the proposed method, four versions of the target domain training set are obtained according to the number of used raw images, *i.e.*, base (B), small (S), tiny (T), and nano (N). SAM-NAT-B swells all original images in the entire NAT2021-*train*, while SAM-NAT-N, SAM-NAT-T, and SAM-NAT-S only randomly sample parts of data with the ratio of about 10.0%, 33.2%, and 50.1%, respectively. Specifically, SAM is adopted for fully automatic training sample swelling, where the post-process of target domain tracking data follows COCO [7]. The qualitative visualization of training samples is shown in Fig. 3. Besides, the quantitative comparison of the training sample numbers between SAM-NAT and NAT2021-*train* is shown in Tab. 1 and discussed in Sec. 4.4 to demonstrate the training sample diversity of the proposed SAM-powered swelling. All the training is complemented with PyTorch on a single NVIDIA A100 GPU and follows [16] with the base tracker [23]. No additional data is introduced.

Evaluation. To validate the tracking robustness in practical UAV applications against complicated challenges [39], [40], [41], the long-term nighttime tracking performance is comprehensively evaluated. From the SOTA nighttime tracking benchmarks, NAT2021-*test* [16] and UAVDark135 [24], the long-term tracking videos are combined following the

rules in the baseline and form **NUT-L**, a comprehensive Long-term Nighttime UAV Tracking benchmark with 43 sequences and 95,274 images. One-pass evaluation is adopted, performances are ranked by success rate, precision, and normalized precision. All the evaluations are complemented with the same platform with training.

4.2 Overall evaluation

This section provides a comprehensive analysis of trackers in nighttime UAV tracking with practical UAV application scenarios. The proposed tracker is based on the SAM-DA framework and is named SAM-DA-Track. According to the version of training data, four trackers are acquired, namely SAM-DA-Track-B, SAM-DA-Track-S, SAM-DA-Track-T, and SAM-DA-Track-N. For fair comparison, SAM-DA-Track-B and other 13 SOTA trackers [16], [23], [27], [28], [42], [43], [44], [45], [46] are overall evaluated on NUT-L.

Results in Fig. 5 show the proposed SAM-DA-Track rank first with a large margin compared to other trackers. Specifically, SAM-DA-Track promotes baseline [16] by 14.1%, 13.4%, and 13.3% on success rate, normalized precision, and precision, respectively. Compared with base tracker [23], SAM-DA-Track raises [23] by 22.9%, 23.6%, and 21.3% on three metrics. SAM-DA-Track presents better adaptability and practicality in variant nighttime conditions. The improvement attributes to the enormous high-quality training samples powered by the excellent zero-shot generalization ability and robustness of SAM.

Figure 6 exhibits some visual comparisons of trackers adopting SAM-DA, the baseline, and the base tracker. SAM-DA raises the nighttime aerial tracking performance of baseline substantially.

4.3 Attribute-based performance

Unlike daytime, objects in actual nighttime UAV tracking scenarios usually experience complex and varied lighting issues. This mainly includes two aspects, the target object undergoes drastic changes in illumination (illumination

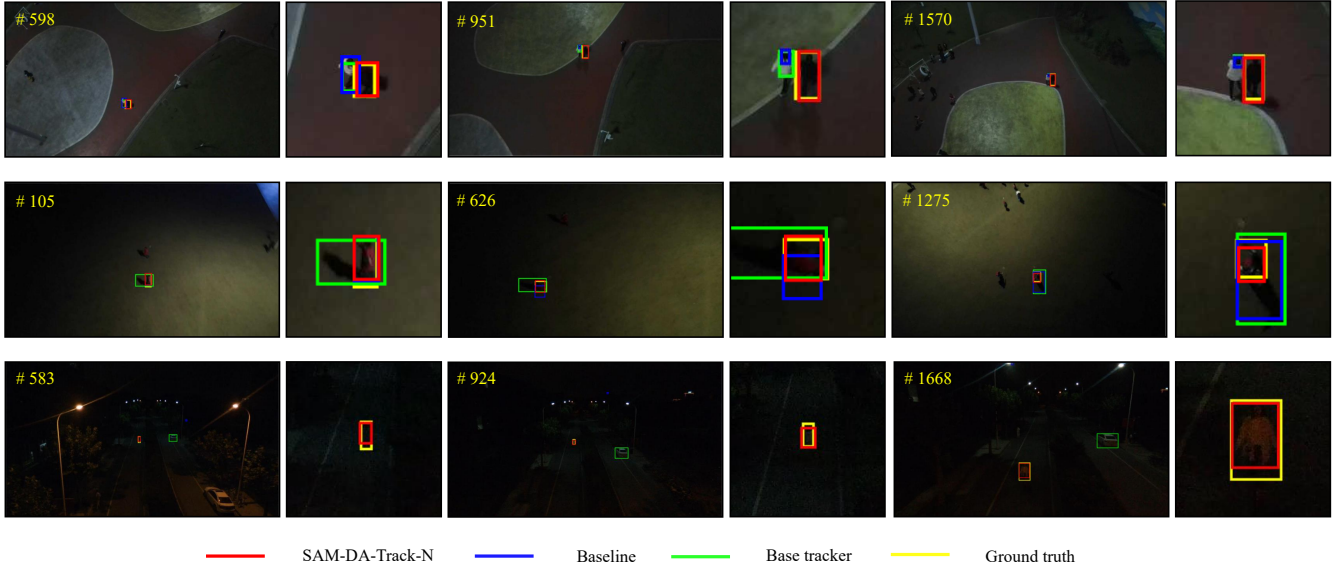


Fig. 6: Visual comparison of the base tracker, the baseline, and the SAM-DA-Track-N in typical night images from NUT-L. With SAM, the proposed fewer-better training contributes to the superior performance of SAM-DA with only 10% of training images of baseline.

TABLE 1: Comparison of SAM-DA and Baseline. With the fewer-better training, SAM-DA can achieve better performance on fewer raw images with more training samples and quicker training. Training duration is obtained on a single NVIDIA A100 GPU. Best performances are highlighted in **bold**. \uparrow denotes higher is better while \downarrow is the opposite.

Method	Target domain dataset	Images	Data proportion	Training samples \uparrow	Traing duration \downarrow	NUT-L		
						AUC \uparrow	P_{Norm} \uparrow	P \uparrow
Baseline [16]	NAT2021- <i>train</i> [16]	276,081	100%	276,081	12h	0.377	0.434	0.498
SAM-DA	SAM-NAT-N	27,745	10.0%	1,608,843	2.4h	0.411	0.471	0.542
	SAM-NAT-T	91,523	33.2%	5,314,760	4h	0.414	0.474	0.545
	SAM-NAT-S	138,242	50.1%	8,042,926	6h	0.419	0.477	0.555
	SAM-NAT-B	276,081	100%	16,073,740	12h	0.430	0.492	0.564

variation, IV) and the object is under extremely low light conditions (low ambient intensity, LAI). Figure 7 presents the performance of SAM-DA-Track and other SOTA trackers against two challenges. Compared with the baseline, SAM-DA-Track achieved a 15.3%, 15.2%, and 15.1% improvement in the three metrics on IV, respectively. While on LAI, SAM-DA-Track promotes the baseline by 12.6%, 10.8%, and 11.1%. The evaluation of the lighting challenges has verified the robustness of SAM-DA-Track against the severe issues for practical nighttime UAV tracking.

Remark 4: As a foundation model for segmentation, SAM presents its superior zero-shot performance even in extremely dark nighttime images. Furthermore, this encouraging phenomenon enables more powerful domain adaptation in other downstream tasks against specific challenges of nighttime domain data.

4.4 Analysis on SAM-powered target domain training sample swelling

Considering the scarcity of nighttime tracking data and the high cost of annotating data under unfavorable lighting conditions, the efficiency of utilizing existing nighttime data has been crucial. The core idea of SAM-DA is to utilize the strong zero-shot generalization ability and robustness

of SAM to produce enormous high-quality training samples in the nighttime tracking data, thus improving day-night domain adaptation.

The high quality of swelled training samples is shown in Fig. 3, where SAM is able to automatically produce pixel-level determined masks with clear boundaries even in the low-light environment. Notably, no low-light image enhancement is required, which is different from the baseline. On the other hand, the number of training samples is greatly enriched, which represents the diversity of swelled training samples. Compared with [47] and [17] used in baseline, SAM is able to discover ‘anything’ potential for tracking. In addition to common objects used in nighttime UAV tracking like cars and people, SAM also includes other valuable tracking candidates, *e.g.*, monitors, and traffic signs in Fig. 3. Therefore, nighttime tracking benefits from the generalization ability and robustness of SAM against complicated scenes.

Enlarged training samples. As shown in Tab. 1, the NAT2021-*train* includes 276,081 training samples in 276,081 training images, with only a single object in each image. A lot of rich and beneficial potential objects remain undiscovered. By contrast, SAM-NAT-N contains 1,608,843 training samples with only 10.0% of training images in NAT2021-

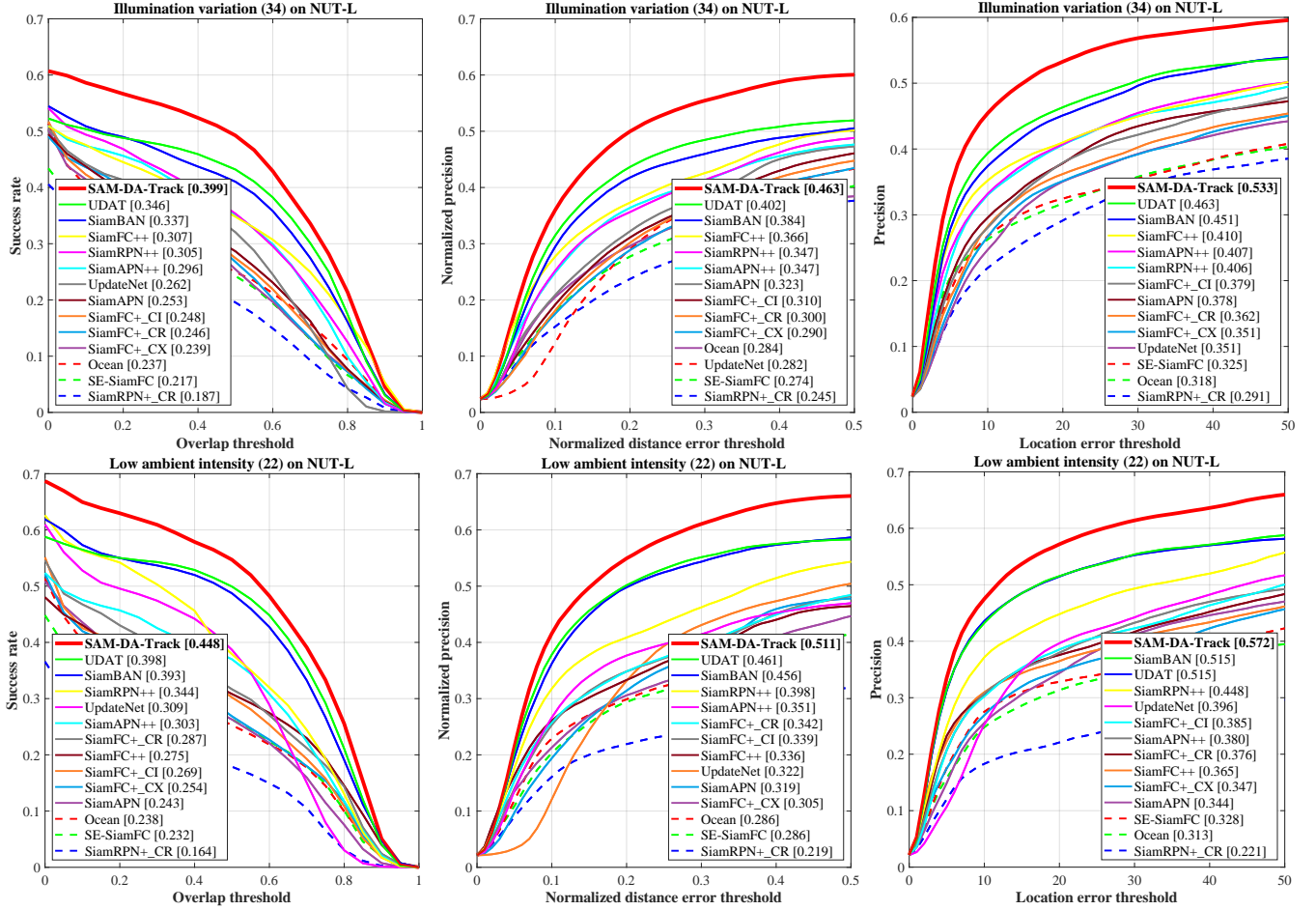


Fig. 7: Evaluation of illumination-related challenges in NUT-L. Attribute to its robustness against dramatic illumination variation and extremely dark environments, the performance of SAM-DA surpasses other SOTA trackers by comparatively large margins.

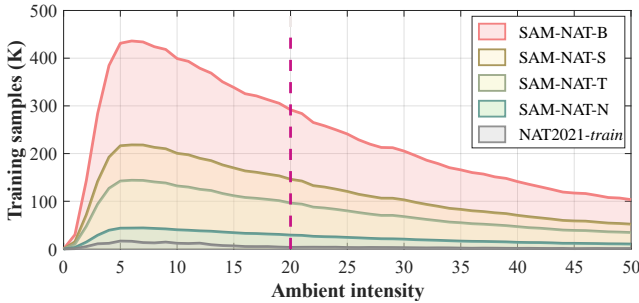


Fig. 8: Ambient intensity (AI) distribution comparison between four versions of SAM-NAT and NAT2021-train. Enormous training samples with diverse lighting conditions are enriched in SAM-NAT with SAM-powered target domain training sample swelling, especially those with AI values less than 20 (the red line), which are considered to be low ambient intensity in [16].

train. The number of training samples of SAM-NAT-N is already 5.8 times of NAT2021-train, as shown in Fig. 9. Besides, SAM-NAT-T uses 33.2% of images and reaches 5,314,760 training samples, while SAM-NAT-S includes

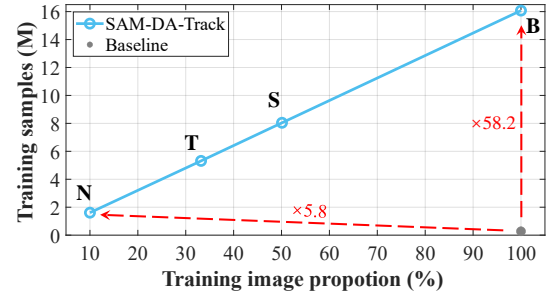


Fig. 9: Quantitative data comparison between SAM-DA and baseline. By SAM-powered target domain training sample swelling, the diversity of training samples in nighttime tracking data achieves significant improvement.

50.1% of images and contains 8,042,926 training samples. SAM-NAT-B uses equal amounts of images with NAT2021-train and contains 16,073,740 training samples, which astonishingly reaches 58.2 times compared to NAT2021-train. Quantitative data comparison between SAM-DA and baseline is shown in Fig. 9.

Enriched lighting conditions. Figure 8 demonstrates the ambient intensity (AI) comparison between SAM-NAT and

NAT-2021-train. The AI value is calculated based on the average lighting conditions of the image patches, where the lower the AI value, the darker the ambient environment in which the target object is located. The patches with AI value of less than 20 are regarded with the attribute of low ambient intensity [16]. Diverse lighting conditions in NAT2021-train are all enriched in SAM-NAT, especially for the training samples with AI value less than 20, *i.e.*, low ambient intensity. The comparison validates that the proposed SAM-powered target domain training sample swelling is able to enrich the distinguished characteristics of the target domain (low light conditions in this case), thus providing a guarantee for improving the knowledge transfer ability of domain adaptation.

4.5 Fewer-better training

Since SAM-DA provides better training samples with fewer data, an intriguing topic is to discuss *can tracker achieves better performance with less training*. This is highly relevant to practical nighttime UAV applications, where the amount of training data is usually limited and quick training is required for timely implementation.

The results in Fig. 10 validate that even with very constrained training image proportion (10.0% on SAM-NAT-N) and training time (about 2.4 hours), SAM-DA-Track can achieve better performance (0.411) than baseline (0.378). It proves the practicality of higher training efficiency with less data. Compared with baseline, SAM-DA-Track achieves a promotion of 9.0% on success rate. With more training data (33.2%, on SAM-NAT-T) and longer training time (about 4 hours), SAM-DA-Track achieves further improvement (0.414). Moreover, on SAM-NAT-S with 50.1% of images and about 6 hours' training, SAM-DA-Track reaches 0.419 AUC score. With SAM-powered target domain training sample swelling on whole data (SAM-NAT-B) and the same training time as baseline, SAM-DA obtains further improvement (0.430). Compared with baseline, SAM-DA-Track achieves the promotion of 14.1%. The fewer-better training evaluation further validates the effectiveness of SAM-powered training sample swelling. It also demonstrates the proposed method is not data-hungry with enormous high-quality training samples, thus more suitable for practical UAV applications.

4.6 Day-night feature distribution

In order to further validate the effectiveness and the domain adaptability of the proposed method, this section includes visualizations of the day-night image features obtained from the base tracker, the baseline, and SAM-DA-Track. Figure 11 shows the visualization results using t-SNE [48]. Comparing the proposed SAM-DA with the base tracker and the baseline, it can be observed that SAM-DA has further reduced the domain discrepancy significantly by leveraging enormous high-quality target domain training samples. As a data-driven method with remarkable zero-shot generalization ability, SAM has been proven that it can be applied for enlarging the target domain training samples for tracking-oriented day-night domain adaptation.

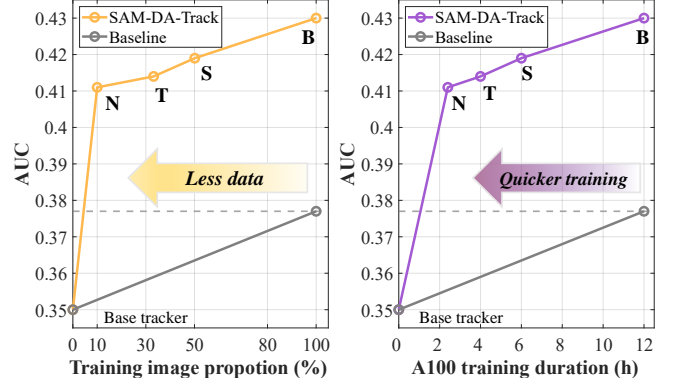


Fig. 10: Feasibility validation of fewer-better training. With fewer data and quicker training, SAM-DA-Track can achieve better performance than the baseline.

5 CONCLUSION

This work is the first study to introduce the superior SAM into the training phase of day-night domain adaptation for nighttime UAV tracking, proposing a novel SAM-powered domain adaptation framework, *i.e.*, SAM-DA. Specifically, the SAM-powered target domain training sample swelling is designed to determine enormous high-quality target domain training samples from every single challenging nighttime image. The above one-to-many generation significantly increases the high-quality target domain training samples for day-night domain adaptation. Consequently, the reliance on the number of raw images required for adaptation training can be decreased, enhancing generalization and preventing overfitting. Extensive evaluation on enormous nighttime videos shows the robustness and domain adaptability of SAM-DA for nighttime UAV tracking. Especially, SAM-DA has achieved better tracking performance with fewer raw training images. To summarize, this work can contribute to the advancement of domain adaptation for object tracking and other vision tasks in various unmanned systems.

6 FUTURE WORK

According to the superior results mentioned above, this work has the potential to be further applied for abundant other applications and extensions as follows.

More nighttime scenarios. This work has proved its adaptation effectiveness with the training and test data in the city scenarios. By virtue of the generalization and robustness of the proposed SAM-DA, this work can be considered for applications in more nighttime and low illumination scenarios, such as villages, wilderness, and even space. This is desirable for promoting the further development of transfer learning in multiple scenes.

More nighttime missions. This work has greatly promoted the day-night domain adaptation with a novel pixel-level one-to-many generation method. SAM-powered target domain training sample swelling provides a new way to solve the expensive and time-consuming annotation for other nighttime missions, including nighttime recognition, nighttime detection, nighttime human pose estimation, and nighttime gesture estimation. This is beneficial for promoting the improvement of other nighttime missions.

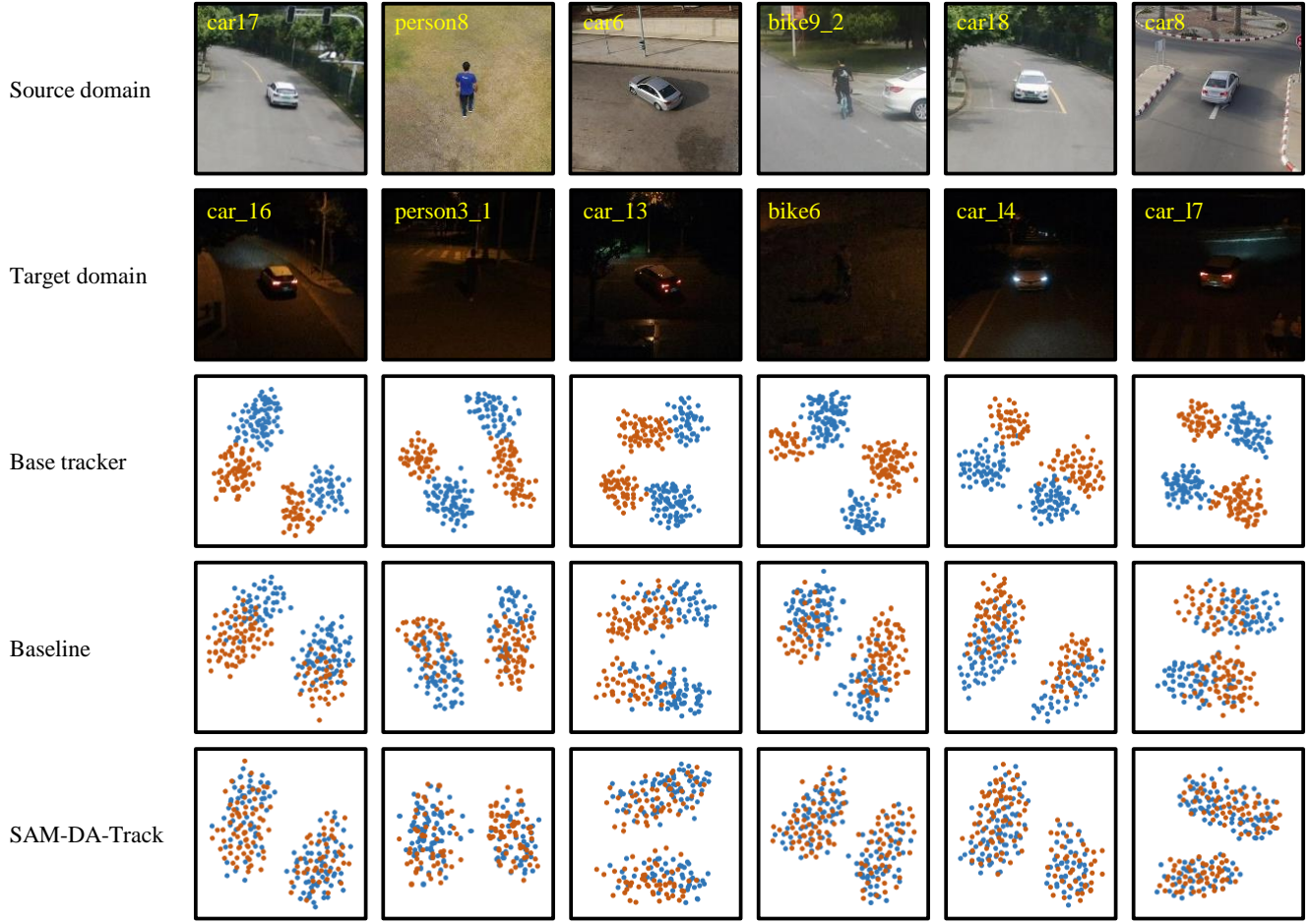


Fig. 11: Feature visualization by t-SNE [48] of day-night similar scenes. The daytime frames are from UAV123 [49] and UAVTrack112 [50], while the nighttime frames are from NUT-L. Blue and orange indicate source and target domains, respectively. The scattergrams depict day-night features from the base tracker, baseline, and SAM-DA-Track. The results show that SAM-DA achieves superior performance to narrow domain discrepancy.

More sensor applications. The work has enhanced the UAV's ability to process low-light images at night. With knowledge transferring and model redesign, this work can be implemented for more sensor applications, such as infrared sensors, depth sensors, and thermal sensors. This is favorable for encouraging further implementation in other sensor applications.

More application platforms. This work is deployed and implemented for UAVs at night with comprehensive experiments. Hence, this work can be studied for more unmanned systems with low computational power, including unmanned surface vehicles, unmanned underwater vehicles, unmanned ground vehicles, and other intelligent robots, etc. This is advantageous for encouraging the advancement of diverse unmanned systems.

REFERENCES

- [1] S. Xuan, S. Li, M. Han, X. Wan, and G.-S. Xia, "Object Tracking in Satellite Videos by Improved Correlation Filters With Motion Estimations," *IEEE Transactions on Geoscience and Remote Sensing*, vol. 58, no. 2, pp. 1074–1086, 2020.
- [2] J. Shao, B. Du, C. Wu, and L. Zhang, "Tracking Objects From Satellite Videos: A Velocity Feature Based Correlation Filter," *IEEE Transactions on Geoscience and Remote Sensing*, vol. 57, no. 10, pp. 7860–7871, 2019.
- [3] L. A. Varga, B. Kiefer, M. Messmer, and A. Zell, "SeaDronesSee: A Maritime Benchmark for Detecting Humans in Open Water," in *Proceedings of the IEEE/CVF Winter Conference on Applications of Computer Vision (WACV)*, 2022, pp. 2260–2270.
- [4] Y. Li, C. Fu, F. Ding, Z. Huang, and G. Lu, "AutoTrack: Towards High-Performance Visual Tracking for UAV With Automatic Spatio-Temporal Regularization," in *Proceedings of the IEEE/CVF Conference on Computer Vision and Pattern Recognition (CVPR)*, 2020, pp. 11 920–11 929.
- [5] H. Fan, H. Bai, L. Lin, F. Yang, P. Chu, G. Deng, S. Yu, M. Huang, J. Liu, Y. Xu et al., "LaSOT: A High-Quality Large-Scale Single Object Tracking Benchmark," *International Journal of Computer Vision*, vol. 129, pp. 439–461, 2021.
- [6] L. Huang, X. Zhao, and K. Huang, "GOT-10k: A Large High-Diversity Benchmark for Generic Object Tracking in the Wild," *IEEE Transactions on Pattern Analysis and Machine Intelligence*, vol. 43, no. 5, pp. 1562–1577, 2021.
- [7] T.-Y. Lin, M. Maire, S. Belongie, J. Hays, P. Perona, D. Ramanan, J. Dollár, and C. L. Zitnick, "Microsoft COCO: Common Objects in Context," in *Proceedings of the European Conference on Computer Vision (ECCV)*, 2014, pp. 740–755.
- [8] E. Real, J. Shlens, S. Mazzocchi, X. Pan, and V. Vanhoucke, "YouTube-BoundingBoxes: A Large High-Precision Human-Annotated Data Set for Object Detection in Video," in *Proceedings of the IEEE/CVF Conference on Computer Vision and Pattern Recognition (CVPR)*, 2017, pp. 7464–7473.
- [9] O. Russakovsky, J. Deng, H. Su, J. Krause, S. Satheesh, S. Ma, Z. Huang, A. Karpathy, A. Khosla, M. Bernstein et al., "ImageNet Large Scale Visual Recognition Challenge," *International Journal of Computer Vision*, vol. 115, pp. 211–252, 2015.
- [10] Z. Cao, C. Fu, J. Ye, B. Li, and Y. Li, "HiFT: Hierarchical Feature

- Transformer for Aerial Tracking,” in *Proceedings of the IEEE/CVF International Conference on Computer Vision (ICCV)*, 2021, pp. 15 457–15 466.
- [11] D. Guo, Y. Shao, Y. Cui, Z. Wang, L. Zhang, and C. Shen, “Graph Attention Tracking,” in *Proceedings of the IEEE/CVF Conference on Computer Vision and Pattern Recognition (CVPR)*, 2021, pp. 9538–9547.
- [12] Q. Wang, L. Zhang, L. Bertinetto, W. Hu, and P. H. Torr, “Fast Online Object Tracking and Segmentation: A Unifying Approach,” in *Proceedings of the IEEE/CVF Conference on Computer Vision and Pattern Recognition (CVPR)*, 2019, pp. 1328–1338.
- [13] H. Zuo, C. Fu, S. Li, J. Ye, and G. Zheng, “DeconNet: End-to-End Decontaminated Network for Vision-Based Aerial Tracking,” *IEEE Transactions on Geoscience and Remote Sensing*, vol. 60, pp. 1–12, 2022.
- [14] J. Ye, C. Fu, Z. Cao, S. An, G. Zheng, and B. Li, “Tracker Meets Night: A Transformer Enhancer for UAV Tracking,” *IEEE Robotics and Automation Letters*, vol. 7, no. 2, pp. 3866–3873, 2022.
- [15] J. Ye, C. Fu, G. Zheng, Z. Cao, and B. Li, “DarkLighter: Light Up the Darkness for UAV Tracking,” in *Proceedings of the IEEE/RSJ International Conference on Intelligent Robots and Systems (IROS)*, 2021, pp. 3079–3085.
- [16] J. Ye, C. Fu, G. Zheng, D. P. Paudel, and G. Chen, “Unsupervised Domain Adaptation for Nighttime Aerial Tracking,” in *Proceedings of the IEEE/CVF Conference on Computer Vision and Pattern Recognition (CVPR)*, 2022, pp. 8886–8895.
- [17] M. Zhang, J. Liu, Y. Wang, Y. Piao, S. Yao, W. Ji, J. Li, H. Lu, and Z. Luo, “Dynamic Context-Sensitive Filtering Network for Video Salient Object Detection,” in *Proceedings of the IEEE International Conference on Computer Vision (ICCV)*, 2021, pp. 1553–1563.
- [18] W. Wang, Q. Lai, H. Fu, J. Shen, H. Ling, and R. Yang, “Salient Object Detection in the Deep Learning Era: An In-Depth Survey,” *IEEE Transactions on Pattern Analysis and Machine Intelligence*, vol. 44, no. 6, pp. 3239–3259, 2022.
- [19] A. Kirillov, E. Mintun, N. Ravi, H. Mao, C. Rolland, L. Gustafson, T. Xiao, S. Whitehead, A. C. Berg, W.-Y. Lo *et al.*, “Segment Anything,” *arXiv preprint arXiv:2304.02643*, pp. 1–30, 2023.
- [20] L. Tang, H. Xiao, and B. Li, “Can SAM Segment Anything? When SAM Meets Camouflaged Object Detection,” *arXiv preprint arXiv:2304.04709*, pp. 1–6, 2023.
- [21] T. Yu, R. Feng, R. Feng, J. Liu, X. Jin, W. Zeng, and Z. Chen, “Inpaint Anything: Segment Anything Meets Image Inpainting,” *arXiv preprint arXiv:2304.06790*, pp. 1–7, 2023.
- [22] S. Roy, T. Wald, G. Koehler, M. R. Rokuss, N. Disch, J. Holzschuh, D. Zimmerer, and K. H. Maier-Hein, “SAM.MD: Zero-Shot Medical Image Segmentation Capabilities of the Segment Anything Model,” *arXiv preprint arXiv:2304.05396*, pp. 1–4, 2023.
- [23] Z. Chen, B. Zhong, G. Li, S. Zhang, and R. Ji, “Siamese Box Adaptive Network for Visual Tracking,” in *Proceedings of the IEEE/CVF Conference on Computer Vision and Pattern Recognition (CVPR)*, 2020, pp. 6667–6676.
- [24] B. Li, C. Fu, F. Ding, J. Ye, and F. Lin, “All-Day Object Tracking for Unmanned Aerial Vehicle,” *IEEE Transactions on Mobile Computing*, 2022.
- [25] B. Li, C. Fu, F. Ding, J. Ye, and F. Lin, “ADTrack: Target-Aware Dual Filter Learning for Real-Time Anti-Dark UAV Tracking,” in *Proceedings of the IEEE International Conference on Robotics and Automation (ICRA)*, 2021, pp. 496–502.
- [26] C. Fu, H. Dong, J. Ye, G. Zheng, S. Li, and J. Zhao, “HighlightNet: Highlighting Low-Light Potential Features for Real-Time UAV Tracking,” in *Proceedings of the IEEE/RSJ International Conference on Intelligent Robots and Systems (IROS)*, 2022, pp. 12 146–12 153.
- [27] B. Li, W. Wu, Q. Wang, F. Zhang, J. Xing, and J. Yan, “SiamRPN++: Evolution of Siamese Visual Tracking With Very Deep Networks,” in *Proceedings of the IEEE/CVF Conference on Computer Vision and Pattern Recognition (CVPR)*, 2019, pp. 4277–4286.
- [28] Z. Cao, C. Fu, J. Ye, B. Li, and Y. Li, “SiamAPN++: Siamese Attentional Aggregation Network for Real-Time UAV Tracking,” in *Proceedings of the IEEE/RSJ International Conference on Intelligent Robots and Systems (IROS)*, 2021, pp. 3086–3092.
- [29] H. Zuo, C. Fu, S. Li, J. Ye, and G. Zheng, “End-to-End Feature Decontaminated Network for UAV Tracking,” in *Proceedings of the IEEE/RSJ International Conference on Intelligent Robots and Systems (IROS)*, 2022, pp. 12 130–12 137.
- [30] C. Fu, M. Cai, S. Li, K. Lu, H. Zuo, and C. Liu, “Continuity-Aware Latent Interframe Information Mining for Reliable UAV Tracking,” *arXiv preprint arXiv:2303.04525*, 2023.
- [31] L. Yao, C. Fu, S. Li, G. Zheng, and J. Ye, “SGDViT: Saliency-Guided Dynamic Vision Transformer for UAV Tracking,” *arXiv preprint arXiv:2303.04378*, 2023.
- [32] X. Wu, Z. Wu, H. Guo, L. Ju, and S. Wang, “DANNet: A One-Stage Domain Adaptation Network for Unsupervised Nighttime Semantic Segmentation,” in *Proceedings of the IEEE/CVF Conference on Computer Vision and Pattern Recognition (CVPR)*, 2021, pp. 15 764–15 773.
- [33] Y. Sasagawa and H. Nagahara, “YOLO in the Dark - Domain Adaptation Method for Merging Multiple Models,” in *Proceedings of the European Conference on Computer Vision (ECCV)*, 2020, pp. 345–359.
- [34] K. He, X. Chen, S. Xie, Y. Li, P. Dollár, and R. Girshick, “Masked Autoencoders are Scalable Vision Learners,” in *Proceedings of the IEEE/CVF Conference on Computer Vision and Pattern Recognition (CVPR)*, 2022, pp. 16 000–16 009.
- [35] A. Dosovitskiy, L. Beyer, A. Kolesnikov, D. Weissenborn, X. Zhai, T. Unterthiner, M. Dehghani, M. Minderer, G. Heigold, S. Gelly *et al.*, “An Image is Worth 16x16 Words: Transformers for Image Recognition at Scale,” in *Proceedings of the International Conference on Learning Representations (ICLR)*, 2021, pp. 1–21.
- [36] A. Vaswani, N. Shazeer, N. Parmar, J. Uszkoreit, L. Jones, A. N. Gomez, L. Kaiser, and I. Polosukhin, “Attention is All You Need,” in *Proceedings of the Advances in Neural Information Processing Systems (NeurIPS)*, 2017, pp. 1–11.
- [37] Y. Ganin and V. Lempitsky, “Unsupervised Domain Adaptation by Backpropagation,” in *Proceedings of the International Conference on Machine Learning (ICML)*, 2015, pp. 1180–1189.
- [38] X. Mao, Q. Li, H. Xie, R. Y. Lau, Z. Wang, and S. Paul Smolley, “Least Squares Generative Adversarial Networks,” in *Proceedings of the IEEE International Conference on Computer Vision (ICCV)*, 2017, pp. 2794–2802.
- [39] C. Fu, K. Lu, G. Zheng, J. Ye, Z. Cao, B. Li, and G. Lu, “Siamese Object Tracking for Unmanned Aerial Vehicle: A Review and Comprehensive Analysis,” *arXiv preprint arXiv:2205.04281*, pp. 1–33, 2022.
- [40] C. Liu, X.-F. Chen, C.-J. Bo, and D. Wang, “Long-term Visual Tracking: Review and Experimental Comparison,” *Machine Intelligence Research*, pp. 1–19, 2022.
- [41] C. Fu, B. Li, F. Ding, F. Lin, and G. Lu, “Correlation Filters for Unmanned Aerial Vehicle-Based Aerial Tracking: A Review and Experimental Evaluation,” *IEEE Geoscience and Remote Sensing Magazine*, vol. 10, no. 1, pp. 125–160, 2021.
- [42] Y. Xu, Z. Wang, Z. Li, Y. Yuan, and G. Yu, “SiamFC++: Towards Robust and Accurate Visual Tracking with Target Estimation Guidelines,” in *Proceedings of the AAAI Conference on Artificial Intelligence (AAAI)*, 2020, pp. 12 549–12 556.
- [43] Z. Zhang and H. Peng, “Deeper and Wider Siamese Networks for Real-Time Visual Tracking,” in *Proceedings of the IEEE/CVF Conference on Computer Vision and Pattern Recognition (CVPR)*, 2019, pp. 4586–4595.
- [44] L. Zhang, A. Gonzalez-Garcia, J. V. D. Weijer, M. Danelljan, and F. S. Khan, “Learning the Model Update for Siamese Trackers,” in *Proceedings of the IEEE/CVF International Conference on Computer Vision (ICCV)*, 2019, pp. 4009–4018.
- [45] Z. Zhang, H. Peng, J. Fu, B. Li, and W. Hu, “Ocean: Object-Aware Anchor-Free Tracking,” in *Proceedings of the European Conference on Computer Vision (ECCV)*, 2020, pp. 771–787.
- [46] C. Fu, Z. Cao, Y. Li, J. Ye, and C. Feng, “Siamese Anchor Proposal Network for High-Speed Aerial Tracking,” in *Proceedings of the IEEE International Conference on Robotics and Automation (ICRA)*, 2021, pp. 510–516.
- [47] C. Li, C. Guo, and C. C. Loy, “Learning to Enhance Low-Light Image via Zero-Reference Deep Curve Estimation,” *IEEE Transactions on Pattern Analysis and Machine Intelligence*, vol. 44, no. 8, pp. 4225–4238, 2022.
- [48] L. Van der Maaten and G. Hinton, “Visualizing Data using t-SNE,” *Journal of Machine Learning Research*, vol. 9, no. 11, p. 2579–2605, 2008.
- [49] M. Mueller, N. Smith, and B. Ghanem, “A Benchmark and Simulator for UAV Tracking,” in *Proceedings of the European Conference on Computer Vision (ECCV)*, 2016, pp. 445–461.
- [50] C. Fu, Z. Cao, Y. Li, J. Ye, and C. Feng, “Onboard Real-Time Aerial Tracking With Efficient Siamese Anchor Proposal Network,” *IEEE Transactions on Geoscience and Remote Sensing*, vol. 60, pp. 1–13, 2022.